A novel clutch coupled drive design for rectification of odometry error: a comparative experimental study

Ammar Nathad Abbas*
Mechanical Engineering Department,
NED University of Engineering and Technology,
Karachi – 75270, Pakistan
Email: ammar.n.abbas@gmail.com
*Corresponding author

Abdul Samad and Shumaila Ahmed
Electronics Engineering Department,
NED University of Engineering and Technology,
Karachi – 75270, Pakistan
Email: abdul.samad@ned.edu.pk
Email: shumailaahmed2014@gmail.com

Umer Abdullah Siddiqui
Mechanical Engineering Department,
NED University of Engineering and Technology,
Karachi – 75270, Pakistan
Email: umer.abdullah99@gmail.com

Abstract: Traversing alignment including straight path motion has been one of the major issues in wheeled mobile robots (WMR). Numerous electronic solutions devised to address the precision issues in locomotion lack to account for the mechanical inadequacy from where the error arises. The issue remains when the WMR is made to follow a route over a longer range as the time accumulated deduced (dead) reckoning error produces enough effect in the action that deviates the WMR from the intended route. The WMR thus suffers from systematic odometry problem and fails to actuate through required trajectory in absence of feedback. Fabrication and controlling of a stupendous design for attaining mechanically synchronised drive and to contribute a cost and energy efficient mechanical structure, independent of complicated sensory feedback and algorithm-based control systems is the superior goal of this research. This publication covers a comparative experimental analysis of conventional proportional integral derivative (PID) controller, an in-practice algorithmic solution, with the suggested design.

Keywords: wheeled mobile robot; WMR; non-holonomic drive; deduced reckoning error; electromagnetic clutch; Vicon motion capture system.

Reference to this paper should be made as follows: Abbas, A.N., Samad, A., Ahmed, S. and Siddiqui, U.A. (2021) 'A novel clutch coupled drive design for rectification of odometry error: a comparative experimental study', *Int. J. Mechatronics and Automation*, Vol. 8, No. 2, pp.62–71.

Biographical notes: Ammar Nathad Abbas is a Mechanical Engineer Graduate from the NED University of Engineering and Technology, and pursuing his Master's in Mechatronic Engineering under Erasmus Mundus Scholarship Program. His objective is to improve the deficiencies of society with technology. His research interest starting from mechatronic system and structures converges to robotics and artificial intelligence. He has several experience under different startups related to STEM education and robotic companies. Further, innovative green energy systems are his another field of interest, which links with his final year project.

Abdul Samad is an Electronics Engineering Graduate from NED University of Engineering and Technology. He has worked as a research assistant and full stack developer at an instrumentation centre and currently serves as an AI engineer at the HEC Technology Development Funded Project of Intelligent and Energy Efficient Fans. He has a strong inclination towards software aspect of field and is exploring computer vision in research. He has earned 'Breakthrough Award' along with fellow team members at Formula Student, UK for the motorsports engineering competition of 2017.

Shumaila Ahmed is an Electronics Engineering Graduate from the NED University of Engineering and Technology, and serving as a software developer at the SkyLin Consultants. Her research interests include, vision analysis, BMI and their application in robotics. Currently, she is working on an AI-based environmental cognition algorithm for visually impaired individuals. She stood second with her project 'Space Rover for path planning and image processing-based obstacle manipulation' in DICE AUTOMOTIVE 2017 in genre of autonomous rovers.

Umer Abdullah Siddiqui is a final year student of Mechanical Engineering at the NED University of Engineering and Technology. His research interests include, continuously variable transmission, innovative concept of rudder, Ram air turbine deploying mechanism, relating lift and thrust for specified airfoil parameters. Currently, he is working on patenting and publishing a research on his innovation of tank truck design with low roll over threshold. He presented his research on tail strike protection devices and won Royal Aeronautical Society Young Person's Lecture Competition 2018. He came 2nd in IET, presented around the world competition in 2018 at Pakistan level.

This paper is a revised and expanded version of a paper entitled 'A novel clutch coupled nonholonomic wheeled mobile robot mechanism to mechanically minimize deduced reckoning error' presented at 2017 IEEE 5th International Symposium on Robotics and Intelligent Sensors (IEEE IRIS2017), Ottawa, Canada, 5–7 October 2017.

1 Introduction

A systematic exposition for the reduction and elimination of deduced reckoning and odometry errors in wheeled mobile robots (WMR) has been one of the most significant research domains since the evolution of autonomous and semi-autonomous WMR for industrial and domestic usage (Rooks, 2002). There are a various error reduction techniques aiming to eliminate the errors caused by the lack of synchronisation that is associated with a generic differential drive actuation mechanism (New et al., 2008). The odometry error integrates over time and causes deviation of the WMR from the desired path over large travel distances. The difference in travel contributed by each wheel of generic differential drives cause the odometry error which can be both systematic and non-systematic (Borenstein and Feng, 1996), the experimental results of this study are used to test systematic and non-systematic error accumulation against a synchronous drive mechanism. Prevailing probes on deduced reckoning error reduction is broadly classified as the one which provides mechanical compensations and the other which account for error evaluation and rectification by means of sensor-data driven feedback algorithms, former provides resolution to causes of errors and latter providing error compensation after it arises (Rooks, 2002). Most errors in the algorithmic solutions occur due to the difference in response to the controller that analyses the traversed difference by each motor. Furthermore, a variety of feedback-based designs with electronic sensory arrangements are existing to reduce the accumulation of errors (Ojeda and Borenstein, 2003; Park et al., 2010; Ahn and Truong, 2009). This paper covers comparative analysis of a general proportional integral derivative (PID)-based feedback algorithm with proposed WMR design as an extension of the previous research which encompasses comprehensive qualitative review of mechanical solutions that are used to minimise systematic odometry errors (Nathad and Rajwani, 2017). This study tends to propose the mechanical compensation of the odometry error by a novel clutch coupled design.

Figure 1 (a) Marker as placed on the top face of conventional WMR (b) Schematic for controlling of PID-WMR (see online version for colours)

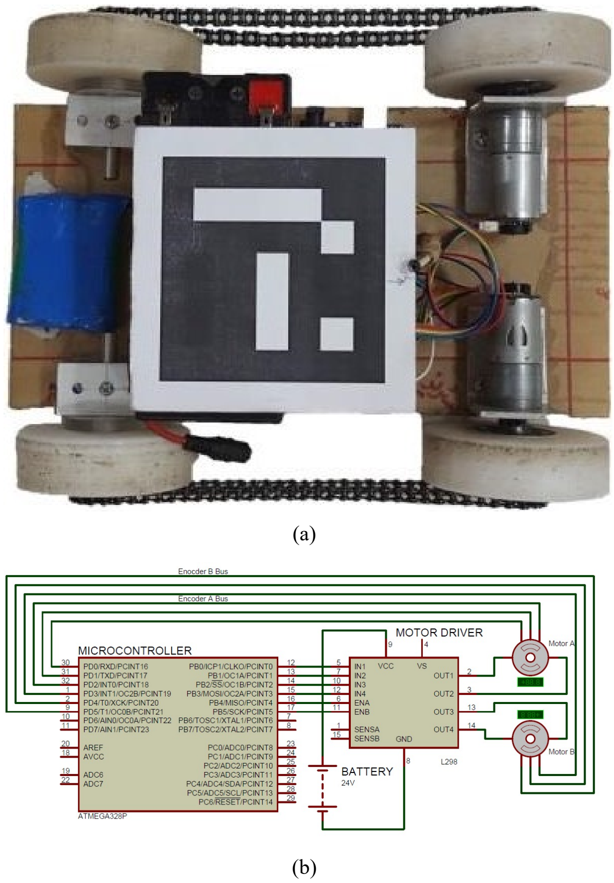

(a)

(b)

The work presented provides quantitative comparison of the feedback-based error reduction to a self-synchronous drive mechanism which mechanically addresses the root cause of the error. The hypothesis put forward is supported by experimental analysis, preceded by the assembly, and modelling of the clutch coupled WMR along with the design and fabrication of a general PID-based robot. Furthermore, the research scope is extended to the error calculation and evaluation, aiming to contribute a cost-effective solution void of complex algorithms to the wide band of researches in regard to deduced reckoning and odometry errors.

2 Literature review

Feedback control-based designs generally make use of simple differential drives whose both wheels are connected directly to DC motors with internal gear arrangements, having no synchronisation between two driving wheels (New et al., 2008), hence offering veer error which is identified by the use of various sensors and compensated by algorithms. Algorithm aided elimination of veering over long distance travel involves complex coding which makes it strenuous to implement and requires extraordinary skill to comprehend. A wide range of feedback aided motion control algorithms in concoction with sensor fusions have been in practice since last two decades including adaptive fuzzy logic controllers to provide efficiently the compensation of these odometry errors, amongst them PID controller is considered to be the most common approach (Visioli, 2001). PID feedback control algorithmic solutions account for deduced reckoning in a non-synchronised drive mechanism. These systems incorporate encoding of the driven entities to introduce feedback for the controller and/or data from various sensors including vision analysis (Subramanian et al., 2006; Cervantes et al., 2004; Dixon et al., 2001; Lima et al., 2016). The controller varies the output to drive accordingly so the error is rectified over time. As evident, these feedback systems efficiency is related to the efficiency of the data acquisition unit, sensor resolution and computational efficiency of the microcontrollers or microprocessors used to implement the feedback logic. Practitioners report deteriorated stability in PID controllers due to these and numerous other reasons (Chong and Kleeman, 1997; Ang et al., 2005; Larsson and Hägglund, 2012; Wang et al., 2002), including tuning inadequacy which involves complex multi-variable tuning algorithms as this control approach are highly dependent on the tuning of control variables which are the controller constants used to vary the actuator output. Design of algorithms for PID controllers and their tuning can be very cumbersome as compared to the achieved optimality (Kim and Cho, 2004; Zhuang and Atherton, 1993). Real-time error analysis and controlled actuation are performed on data acquired in runtime from electronic odometers which are prone to environmental and systematic errors producing erroneous data which requires filtering in order to avoid deluded analysis (Seifert and Camacho, 2007). Numerous techniques are used to filter sensor data including probabilistic filtering, these filtering algorithms add to the complexity of feedback controllers ranging from less complex smoothing/moving average filters to more complex Kalman filters (Ahn and Truong, 2009). The implementation of the PID controller is least complex as compared to the implementation of other feedback-based control algorithms such as fuzzy logic controller (Lee et al., 2002), predictive controller (Raffo et al., 2009), or adaptive controller (Henaff et al., 1994). These controllers are used widely to address the odometry error in standalone configurations as well as in cocktail along with contortions of composite filters to tackle nonlinearity of the feedback loop. On other hand, researches have been reported on mechanical compensation for veer and off-course error proposing numerous synchronous drive mechanisms (Nathad and Rajwani, 2017), this study is an extension of author's* previous research on the comparative analysis of the proposed WMR to these mechanical solutions. This paper presents a novel clutch coupled design of WMR for mechanically addressing odometry error in a comparative analysis with the PID approach implemented to a differential drive design. The conventional model comprises of a four-wheel drive (4WD) using two DC geared motors with encoders *(JGA25-371B)*, one driving each side of the structure. The motors are positioned at the rear part that further coupled the rear wheels to transfer 100% torque at the same rate as the motors. The front drive contains free wheels that are connected with the rear wheels through a sprocket chain arrangement resting on the fixed steel rods as shown in Figure 1(a). The robot electronics of PID-based robot uses an open-source Arduino microcontroller implementing an open-source PID autotune library (Beauregard, 2013) used in order to frame a strategic algorithm for tuning of constants. Figure 1(b) represents the design schematic for the conventional WMR. The microcontroller board takes input from encoders and motors are controlled by a motor driver. Both contenders have been intelligently designed to be identical in terms of physical parameters represented in Table 1. The weights are adjusted by placing dead mass at the approximate centre of the robot bases.

Table 1 Physical parameters for contenders

Length (cm)	*Base width (cm)*	*Total width (cm)*	*Wheel width (cm)*	*Wheel radius (cm)*	*Weight (kg)*
30.226	14.986	21.336	21.336	4.318	3.8

3 Proposed non-holonomic clutch coupled WMR

The section encompasses structural anatomy and steer control methodologies of proposed WMR, including both mechanical and electronic aspects of modelling, assembly and controlling.

3.1 Fabrication and assembly

The chassis where all the components were assembled was chosen to be of 8 mm thick acrylic. Modular assembly approach has opted so that each element could be replaced or disassembled for troubleshooting independently, without dismantling the whole structure. Stainless steel axle having a radius of 8 mm; functioned as the front and back axles, is used to align the left and right sides of the wheel assembly on the base. Coupling is made of mild steel rolled down by means lathe machine according to the required dimensions to give mechanical flexibility in movement and for easy assembly of the back axle. High torque DC geared motors transfer the torque to drive the structure which is transferred by means of the front and back axles. For driving and achieving the desired turning tasks, two independent *Pittman* DC geared motors of high torque were used. These two motors are positioned for adequate independent transmission to the front and back axle. The use of electromagnetic clutches the makes the front and back drives independent were extracted from an old photocopier. The basic design, structure, and working of an electromagnetic clutch are explained in the design section of the related paper (Nathad and Rajwani, 2017). The clutches are operated so as to achieve maximum engagement for efficient torque transfer. Amplified current from the L293D motor driver module is used to engage the clutches when required. Clutches, when disengaged, allow free movement of the respective transmission. The front transmission use bevel gears rendering control objective of rotating the bot on its own axis by allowing the left and right side drive to move with the speed of front motor in opposite directions. The gear is fixed to the front motor that transfers torque to the two pinions that are further connected to the clutches used to drive both sides of the drive in alternate directions. To strengthen the bevel gear drive, bushes of mild steel turned down on lathe machine are welded to the pinions' bore. The pinions alignment is achieved using a free axle passing within the bore of pinions. To transfer the torque from the back motor to the back axle and to transfer the drive within the front and back wheels, a chain and sprocket arrangement of motorbike engine is used. The back axle further connects with the two rear clutches that are integrated within the wheels. Wheels are made of soft nylon with a radius of 4.318 cm fabricated on lathe machine as per the requirements with the desired bore to integrate the clutch head into the wheel. The final fabricated and assembled structure along with its dimension is shown in Figure 2(a).

3.2 Electronic schematic

Figure 2(b) provides the control schema of the conventional WMR. The clutch drive consists of a metal-oxide-semiconductor field-effect transistor (MOSFET)-based driver module to operate clutches alternatively at 24 VDC. The driver is controlled at the logic level voltage by the micro-controller and it switches the clutches over the high voltage supply. The ground line connection is made common between both voltage levels.

3.3 Kinematics

The kinematics equations involved in actuation of the WMRs accounts for the basic design difference and motion inadequacy in conventional WMR and its rectification in NC design, Figure 3(a). In conventional WMRs, the net velocity offered by the right segment is not equivalent to net velocity offered by the left segment, as the drive wheel and driven wheels on each side are entirely independent of each other. Due to this non-synchronous motion, velocity mismatch at any instance of time result in in-compensable deviation from the desired line of motion and therefore requires assistive feedback algorithms. The curved trajectories are also encoder aided with no with velocity control. The non-conventional WMR offers a mechanical synchronisation in all instances, hence during forward motion, the net velocity of right-hand side (RHS) is equal to the net velocity of left-hand side (LHS), hence theoretically follows an ideal straight path. The velocities on RHS are equal and opposite to LHS in on-axis rotation-enabling consistent rotational capabilities. Similarly, the conventional design offers relative velocity difference on both halves to enable curved trajectories and sharp turns.

Figure 2 (a) Top view of the assembled structure of NC-WMR (b) Control schematic for clutch coupled WMR (see online version for colours)

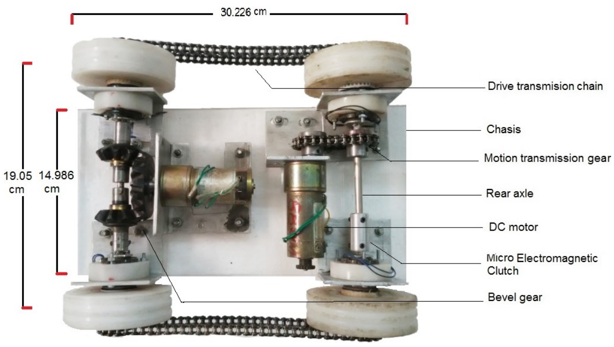

(a)

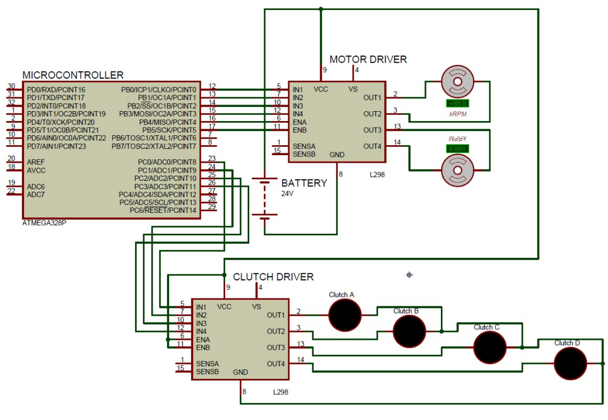

(b)

3.4 Mechanical schematic of various control objectives

Figure 3(b) explains various control objectives of the proposed 4WD that are commonly required in a WMR to perform different tasks. The forward and reverse motion is controlled by the rear motor only, which, when moved in an anticlockwise direction produces forward motion and with a clockwise direction controls the reverse motion of the WMR. To transfer the motion to the wheels, the rear clutches are engaged to transfer the torque from the motor to the rear drive wheels. The front wheels are driven by the rear wheels that are connected through a chain and sprocket arrangement. Since only a single motor controls the speed of all the four wheels, therefore the wheels are synchronised with one another, ideally, neglecting the slippage and friction error. To achieve the on-axis rotation, the two sides of the drives must be powered with the same speed but in an alternate direction. The front motor controls the right and left actuation through the clockwise and anticlockwise rotation respectively to rotate the structure on its own axis. The required motion and synchronous speed are attained by the use of single motor transferring torque through a bevel gear and pinion arrangement. The front clutches are engaged for the transfer of mechanical power to the front wheels that further drives the rear wheels. The sharp turn is controlled by powering the single side of the structure and keeping the other side at rest. With the back motor powered in the anticlockwise direction and one of the rear clutches engaged, the desired short left and right curves are attained. The front wheel of the respective side is driven by the engaged rear wheel.

In order to drive the robot with larger curves, the two sides of the structure must be powered through a relative speed with the structure turning in the direction opposite to the side with the greater velocity. Therefore, to achieve the speed difference, both the motors were powered in respective directions to achieve the forward motion and alternate clutches are engaged. The rear motor provides the greater velocity to the desired side along with the respective clutch engaged and the front motor provides the lower speed to the other side with the alternate clutch engaged. The free wheels for both the sides are driven by the engaged wheel. The experimentation for curved trajectories is beyond the scope of this research and will be addressed in future extensions.

3.5 Braking and free-wheel stopping conditions

An additional functionality of such application of clutches was discovered during testing, it was found that braking capability can be achieved by engaging all the clutches together after the termination of torque transfer. The experimental comparison of the results of free-wheel and braking conditions are given in Figures 4(a) and 4(c), on the other hand for conventional design, the commonly used braking mechanism is to use gradual decrement in pulse width modulus (PWM) or by signaling the motor to rotate clock and anticlockwise alternatively for a fraction of second.

Figure 3 (a) Kinematics of the contenders, left: conventional, right: non-conventional (b) Mechanical schematic and control strategies aided with the nomenclature of pictorial representation

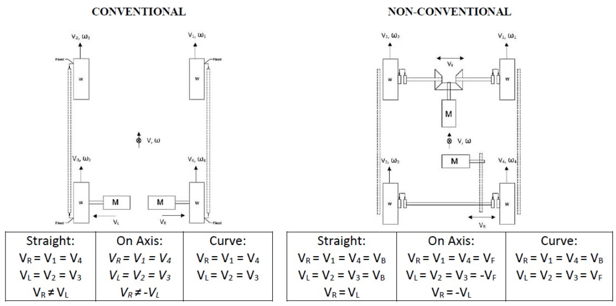

(a)

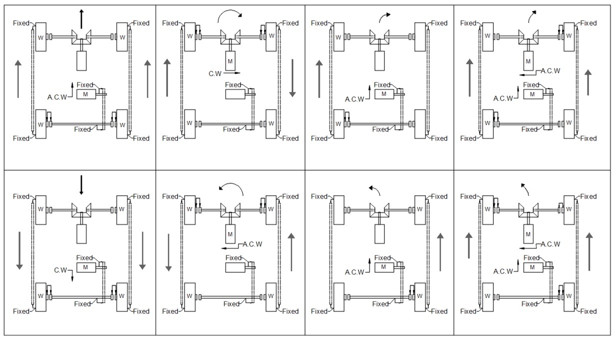

(b)

4 Experimental analysis and error estimation

In this section, the experiments along with their significance and necessary nomenclature for inference of results are discussed. The tests requisites travel over defined trajectory and the computational results give the deviation which is used to calculate error(s) to provide basis of further comparative hypothesis as discussed in Section 5. All tests were performed on motion capture system $Mubassir$ at Intelligent Mobile Robotics Lab Pakistan Air Force Karachi Institute of Economics and Technology (PAF-KIET), Pakistan. The facility is similar to Vicon motion capture system (Windolf et al., 2008). The results are generated in form of data points which were further processed using a multi-paradigm numerical computing environment, Matrix Laboratory (MATLAB). The testing system uses a ceiling mount camera to capture movement on a high frame rate, further processed on a Raspberry-Pi microcomputer to produce data points. The camera only tracks a specified marker pattern placed on the top face of WMR as shown in Figure 1(b). These data points then were used to calculate motion and positioning parameters presented in this research study. All tests were performed on the same day and same time for both conventional PID-based and non-holonomic clutch coupled design. The system efficiency, test floor, and other conditions were identical for both robots involved in the comparative analysis.

Figure 4 Linear regression for straight path repeatability, (a) braking iterative regression, top: PID, bottom: NC (b) (d) top: time variant deviation from the desired path, bottom: averaged error (c) free-wheel iterative regression, top: PID, bottom: NC (see online version for colours)

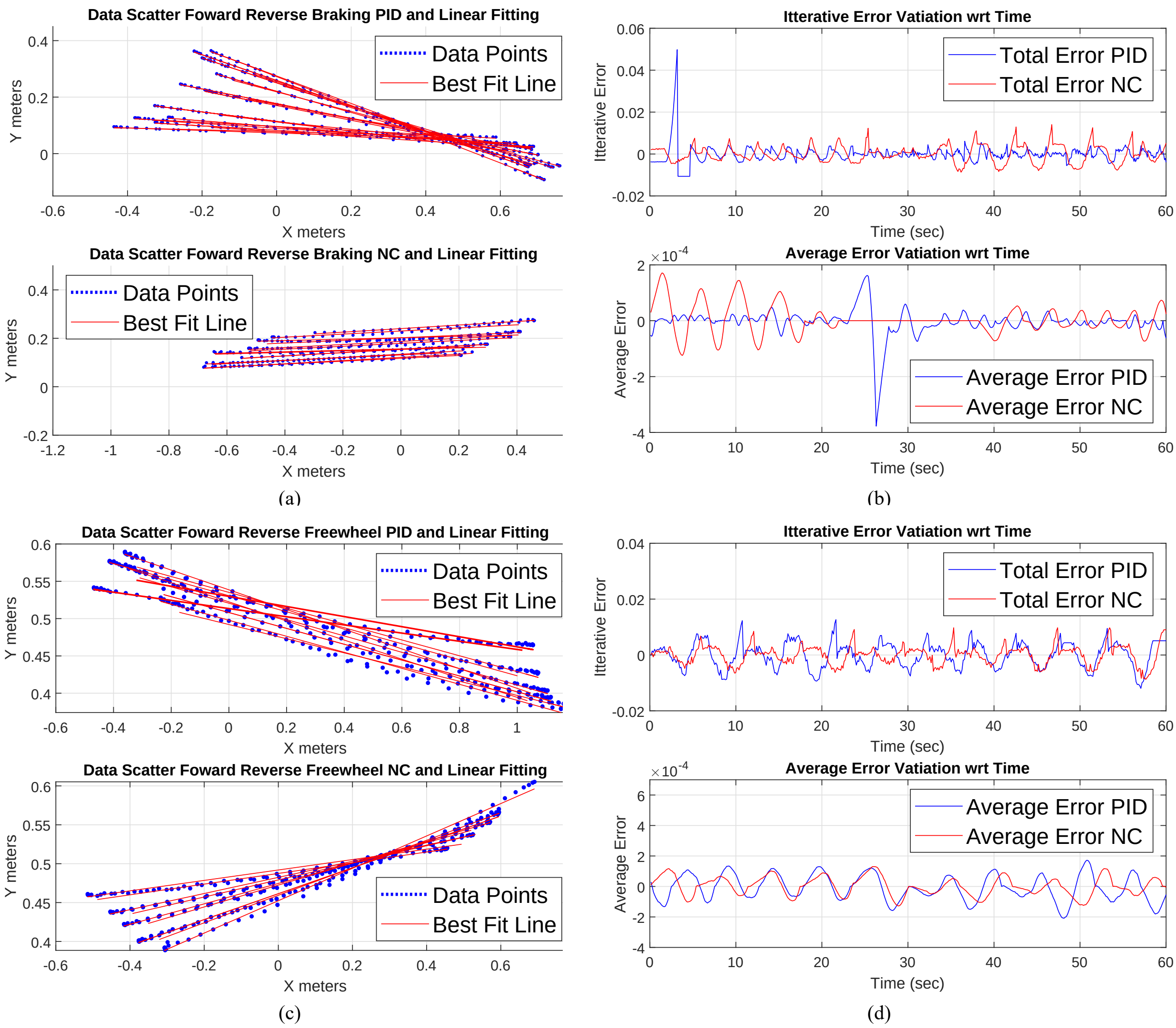

Figure 5 Time varying heading error graphs for straight path precision, (a) braking (b) free-wheel, top: absolute error, bottom: average error (see online version for colours)

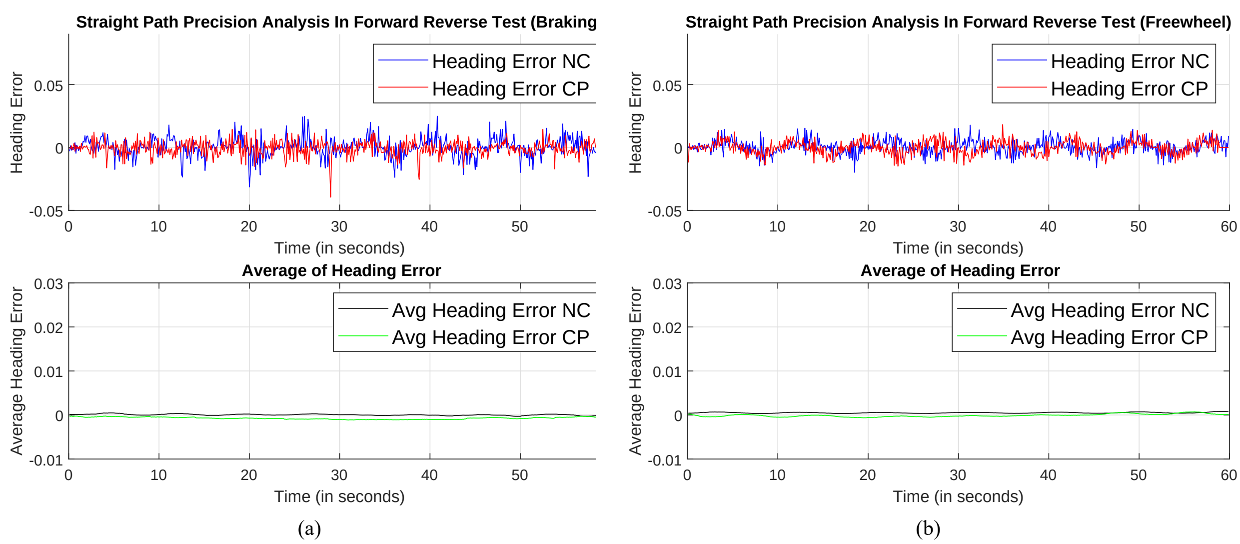

Figure 6 Curve fitting and error evaluations for circular and on-axis tests, (a) circular trajectory of both PID and NC (b) on-axis curve fitting results, left: PID, right: NC (see online version for colours)

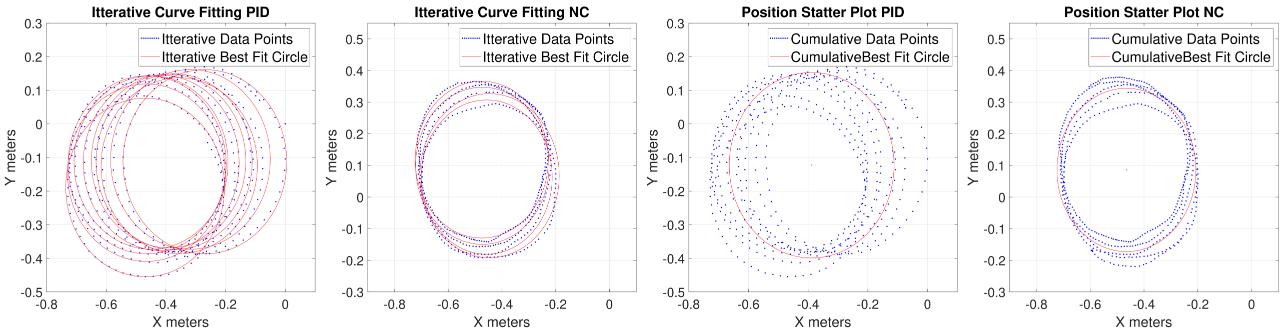

(a)

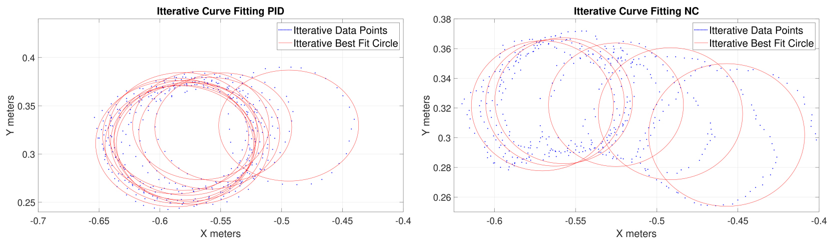

(b)

Figure 7 (a) Shift in position during circular test (b) Shift in position during on-axis test, left: PID, right: NC-WMR (see online version for colours)

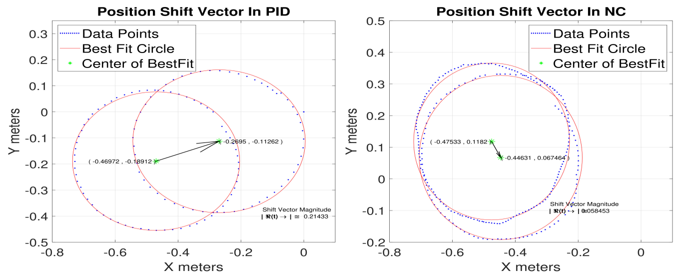

(a)

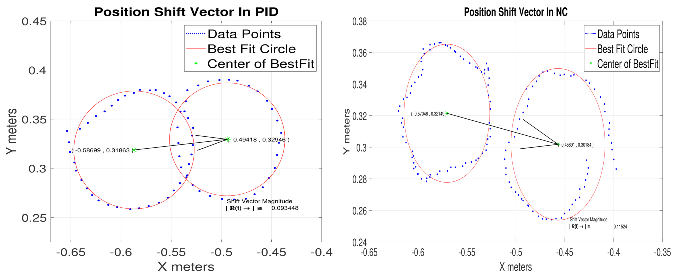

(b)

4.1 Forward-reverse braking and free-wheel linear tests

The forward and reverse iterative actuation analysis was performed aiming to compare the repeatability and path precision. This test was performed under two conditions braking and free-wheel as discussed in Section 3. The desired motion was recurring straight lines.

4.1.1 Path precision in linear motion

For linear motion along any straight path [equation (1)], the change in heading, i.e., the change in the slope of line of motion [equation (2)], should be ideally zero.

$$Y = mX + b \tag{1}$$

$$M = \frac{y_2 - y_1}{x_2 - x_1} \tag{2}$$

For error analysis, path precision is then quantified by means of linear regression for each separate forward and reverse motion, here the main concern is that whether the relationship pattern between values of dependent variables can be described as a straight line given as equation (3), Where β is the regression coefficient and is the change in Y associated with a one-unit change in X, formula for β is given by equation (4). Also, γ is called residual, error term to account for variations of the time series univariate data equation (5), and used for time-variant error plotting.

$$\hat{\mathbf{Y}} = \beta X + a + \gamma \tag{3}$$

$$\beta = \frac{\sum(Y - \overline{Y})(X - \overline{X})}{\sum(X - \overline{X})^2} \tag{4}$$

$$\gamma = Y_i - (\hat{\mathbf{Y}}_i) \tag{5}$$

$$Y_n = \frac{1}{M} \sum_{(k=0)}^{(M-1)} X_{[n-k]} \tag{6}$$

The positive values of error shows that fitting is overestimated and negative values show fitting is underestimated, hence directly equated as the deviation from a precise path Figures 4(b) and 4(d) (top), to eliminate the effect of random shocks from the error analysis and to eliminate the erroneous effects of white noise, Figures 4(b) and 4(d) (bottom) gives the moving average of the error values Y_n using equation (6).

4.1.2 Repeatability in linear motion

For the motion of each robot in linear positioning test Figures 4(a) and 4(c) change in heading is evident in both cases for both PID and clutch coupled WMR providing grounds for repeatability analysis, the error evaluation graphs in Figure 5 show estimate comparative analysis for each case. Change in time variant heading data (in radians) is calculated for each data point indicating the deviation in motion along the path cumulatively for entire test duration, i.e., 60 seconds [equation (7)].

$$Heading\ error(\epsilon) = \theta_n - \theta_{(n-1)} \quad (7)$$

Average heading error [equation (8)], Figures 5(a) and 5(b) (bottom) is calculated from the slope of best fitting equations, each forward and reverse motion is estimated by linear fitting [equation (3)], and the change in slope of each equation determines the average change in direction per forward and reverse movement.

$$Averaged\ heading\ error(\epsilon) = \beta_n - \beta_{(n-1)} \quad (8)$$

4.2 Circular trajectory and on-axis rotation tests

For circular trajectory both robots were made to continually travel the circumference of a hypothetical circular path keeping speed constant for 60 seconds. For on-axis rotational analysis, the robots were made to actuate in the anticlockwise direction for the same amount of time.

4.2.1 Path precision in circular and on-axis motion

The path precision in circular trajectories is then quantified using circle fit algorithm developed by Bucher (2004) for each complete rotation Figures 6(a) (1, 2) and 6(b), to evaluate iterative error and complete data set Figures 6(a) (3, 4) for average deviation, here the concern is that whether the relationship pattern between data points can be described by equation of a circle given by equation (9). The data points were estimated by equation (10), to account for further error evaluations, γ is called residual, error term to account for variations of univariate time series data given using equation (11),

$$(X - h)^2 + (Y - k)^2 = R^2 \quad (9)$$

$$(\hat{\mathbf{X}} - h)^2 + (\hat{\mathbf{Y}} - k)^2 = R^2 + \gamma \quad (10)$$

$$\gamma = Y_i - (\hat{\mathbf{Y}}_i) \quad (11)$$

More comprehensively, the distance of each data point should be equal to radius of its best fitting for an error-free accurate circular path for both average deviation and iterative cases, hence for each data point the amount by which the Euclidean distance is greater or less than radius value is the iterative error and average error as shown in Figure 6.

4.2.2 Repeatability in circular trajectory and on-axis rotation

The repeatability of circular trajectory and axis rotation is directly related to the shift in the centre of the circular path, this methodology is opted to quantify repeatability, higher the magnitude of position shift vector lower the repeatability of the experiment. Figure 7 indicates the shift in centre of first and last iteration for both PID-based robot and NC-WMR the shift in position increases with time or number of rotations hence the shift vector [equation (12],

$$|R\rightarrow| = \sqrt{(x_1 - x_2)^2 + (y_1 - y_2)^2} \quad (12)$$

5 Results and inference

The hypothesis and results are derived on basis of graphical models of each of the experiments conducted. The repeatability and precision of the path are key factors to estimate efficiency. For simplicity, in this very short paper position error drives precision and repeatability is analysed using trajectory error.

The curve fitting and linear regression results are taken as the true measurements and vision-based positioning system data used to estimate position errors, which are defined as the Euclidean distance between former and latter. The test results in the previous sections give orderly error accumulation information and consistent deviation pattern that is used for qualitative comparison between the conventional and non-conventional WMR. Figure 4(a) (top) shows huge variation in the heading of the rover and the intersection on linear iterations indicate inconsistent repeatability and deviation from the straight path over time while resulting parallel lines in Figure 4(a) (bottom) infer to produce least heading variations and high repeatability, however, the data fitting was found to be inconsistent indicating low path precision. Figure 4(c) (top) shows improved results for PID with lesser slope variations but the data itself tends to deviate from its best fitting showing a low degree of negative correlation. Figure 4(c) (bottom) on the other hand, tends offers a higher degree of positive correlation with a compromised slope consistency, however, the variations were found to be less than the variations in PID Figure 4(a) (top). The estimated path precision errors Figures 5(a) and 5(b) further clarify the observation. Path precision error plot for the straight paths and the averaged values manifest that the magnitude of error in conventional PID robot is more as compared to clutch coupled non-conventional WMR design. For circular test results, the data values for NC and PID WMR by vision-based positioning system closely match the fitting curves, indicating high path precision in both, however, the data dispersion as shown in Figure 6(b) (bottom) is evident to be higher in PID robot indicting lesser repeatability, while clutch coupled design provides better traction force keeping motion path less deviated. The position displacement, given by the displacement vector $\overrightarrow{R}$ also indicates that the position shift or shift in the centre of the circle is considerably low in comparison to the circular trajectory of PID-based rover. Whereas, for on-axis rotation Figure 6(b) (right), it is observed that the proposed design lack consistent motion and centre of rotation to deviate greatly from the initial position, in contrast to the PID based WMR Figure 6(b) (left) exhibit lesser deviation indicating better repeatability and adequate path precision.

In addition to the derived results, a crucial observation was made during experimentation. It was found that the proposed clutch coupled design has superlative power efficiency. The consumption of PID-based WMR was found to be significantly greater as two motors are required to power at same time, whereas, the proposed design a single motor to be powered at an instance.

6 Conclusions and future research

The paper provides a comparative study and detailed analysis to weigh the proposed mechanical solution of veer and odometry errors against conventional complex algorithmic feedback PID controller. The research sheds light that the mechanical compensation is fairly adequate considering the fact that the complexity of algorithmic solutions increase when data filtering and linearisation modules are incorporated, intensifying the nexus beyond feasibility of small-scale application. The proposed design can be a good alternate to algorithm-based reckoning solutions as the design was found to effectively address the error accumulation without the extra hustle of complex programming for feedback algorithms. The future research includes precise clutch engagement techniques and experimental analysis of their effects in closed loop trajectories and arbitrary paths with the inclusion of quantitative power consumption analysis and comparison. Further, research also spans improvement and modification of current design, based on the notion of presented results to mechanically reduce non-holonomic constraints and produce a robust solution for industrial applications, which if successful, will be a groundbreaking advancement in the positioning of WMRs with least odometry.

Acknowledgements

The authors would like to acknowledge Intelligent Mobile Robotics Lab PAF-KIET, for providing the testing facility, also they would like to pay gratitude to fabrication workshop NED-UET for providing facility and assistance in fabrication and assembly of contenders presented in this paper.

References

Ahn, K.K. and Truong, D.Q. (2009) ‘Online tuning fuzzy pid controller using robust extended kalman filter’, *Journal of Process Control*, Vol. 19, No. 6, pp.1011–1023.

Ang, K.H., Chong, G. and Li, Y. (2005) ‘PID control system analysis, design, and technology’, *IEEE Transactions on Control Systems Technology*, Vol. 13, No. 4, pp.559–576.

Beauregard, B. (2013) *Arduino PID Autotune Library*, Playground [online] http://playground.arduino.cc/Code/PIDLibrary (accessed 2017).

Borenstein, J. and Feng, L. (1996) ‘Measurement and correction of systematic odometry errors in mobile robots’, *IEEE Transactions on Robotics and Automation*, Vol. 12, No. 6, pp.869–880.

Bucher, I. (2004) *Circle Fit: Circfit. M*, Computer Program, Mathworks.

Cervantes, I., Garrido, R., Alvarez-Ramirez, J. and Martinez, A. (2004) ‘Vision-based PID control of planar robots’, *IEEE/ASME Transactions on Mechatronics*, Vol. 9, No. 1, pp.132–136.

Chong, K.S. and Kleeman, L. (1997) ‘Accurate odometry and error modelling for a mobile robot’, in *IEEE International Conference on Robotics and Automation, Proceedings*, IEEE, Vol. 4, pp.2783–2788.

Dixon, W.E., Dawson, D.M., Zergeroglu, E. and Behal, A. (2001) ‘Adaptive tracking control of a wheeled mobile robot via an uncalibrated camera system’, *IEEE Transactions on Systems, Man, and Cybernetics, Part B (Cybernetics)*, Vol. 31, No. 3, pp.341–352.

Henaff, P., Milgram, M. and Rabit, J. (1994) ‘Adaptive neural control in mobile robotics: experimentation for a wheeled cart’, in *IEEE International Conference on Systems, Man, and Cybernetics, Humans, Information and Technology*, IEEE, Vol. 2, pp.1139–1144.

Kim, D.H. and Cho, J.H. (2004) ‘Intelligent tuning of PID controller with disturbance function using immune algorithm’, in *2004 IEEE International Conference on Computational Intelligence for Measurement Systems and Applications, CIMSA*, IEEE, pp.109–114.

Larsson, P. and Hägglund, T. (2012) ‘Comparison between robust PID and predictive PI controllers with constrained control signal noise sensitivity’, in *IFAC Conf. Advances in PID Control PID*, Vol. 12, No. 2, pp.175–180.

Lee, C-H., Lee, Y-H. and Teng, C-C. (2002) ‘A novel robust PID controller design by fuzzy neural network’, *Asian Journal of Control*, Vol. 4, No. 4, pp.433–438.

Lima, T.A., do Nascimento Forte, M.D., Nogueira, F.G., Torrico, B.C. and de Paula, A.R. (2016) ‘Trajectory tracking control of a mobile robot using Lidar sensor for position and orientation estimation’, in *2016 12th IEEE International Conference on Industry Applications (INDUSCON)*, IEEE, pp.1–6.

Nathad, A. and Rajwani, J. (2017) 'A novel clutch coupled nonholonomic wheeled mobile robot mechanism to mechanically minimize deduced reckoning error', in *2017 IEEE International Symposium on Robotics and Intelligent Sensors (IRIS)*, IEEE, pp.284–289.

New, A.A., Zan, A.A. and Aung, W.P. (2008) 'Control system consideration of IR sensors-based tricycle drive wheeled mobile robot', *International Journal of Computer, Information, Systems Science and Engineering*, Vol. 2, No. 1, pp.30–36.

Ojeda, L. and Borenstein, J. (2003) 'Reduction of odometry errors in over-constrained mobile robots', in *Unmanned Ground Vehicle Technology V*, International Society for Optics and Photonics, Vol. 5083, pp.431–440.

Park, B.S., Yoo, S.J., Park, J.B. and Choi, Y.H. (2010) 'A simple adaptive control approach for trajectory tracking of electrically driven nonholonomic mobile robots', *IEEE Transactions on Control Systems Technology*, Vol. 18, No. 5, pp.1199–1206.

Raffo, G.V., Gomes, G.K., Normey-Rico, J.E., Kelber, C.R. and Becker, L.B. (2009) 'A predictive controller for autonomous vehicle path tracking', *IEEE Transactions on Intelligent Transportation Systems*, Vol. 10, No. 1, pp.92–102.

Rooks, B. (2002) 'Mobile robots walk into the future', *Industrial Robot: An International Journal*, Vol. 29, No. 6, pp.517–523.

Seifert, K. and Camacho, O. (2007) 'Implementing positioning algorithms using accelerometers', *Freescale Semiconductor*, pp.1–13.

Subramanian, V., Burks, T.F. and Arroyo, A. (2006) 'Development of machine vision and laser radar based autonomous vehicle guidance systems for citrus grove navigation'. *Computers and Electronics in Agriculture*, Vol. 53, No. 2, pp.130–143.

Visioli, A. (2001) 'Tuning of pid controllers with fuzzy logic', *IEEE Proceedings-Control Theory and Applications*, Vol. 148, No. 1, pp.1–8.

Wang, Q-G., Hang, C., Yang, Y. and He, J. (2002) 'Quantitative robust stability analysis and PID controller design', *IEEE Proceedings-Control Theory and Applications*, Vol. 149, No. 1, pp.3–7.

Windolf, M., Götzen, N. and Morlock, M. (2008) 'Systematic accuracy and precision analysis of video motion capturing systems – exemplified on the vicon-460 system', *Journal of Biomechanics*, Vol. 41, No. 12, pp.2776–2780.

Zhuang, M. and Atherton, D. (1993) 'Automatic tuning of optimum PID controllers', in *IEEE Proceedings D (Control Theory and Applications)*, IET, Vol. 140, No. 3, pp.216–224.